Towards more robust hydroacoustic estimates of fish abundance in the presence of pelagic macroinvertebrates

Rebecca A. Dillon[1*], Joseph D. Conroy[2], Lars G. Rudstam[3], Peter F. Craigmile[4], Doran M. Mason[5], and Stuart A. Ludsin[1]

[1]*Aquatic Ecology Laboratory, Department of Evolution, Ecology, and Organismal Biology, The Ohio State University, Columbus, OH 43212, USA*
[2]*Inland Fisheries Research Unit, Division of Wildlife, Ohio Department of Natural Resources, Hebron, OH 43025, USA*
[3]*Department of Natural Resources and the Cornell Biological Field Station, Cornell University, Ithaca, NY 14850, USA*
[4]*Department of Statistics, The Ohio State University, Columbus, OH 43210, USA*
[5]*Great Lakes Environmental Research Laboratory, National Oceanic and Atmospheric Administration, Ann Arbor, MI 48108, USA*

*Corresponding author: *tel: + 1 614 292 1613; fax: +1 614 292 0181 e-mail: dillon.361@osu.edu* (https://orcid.org/0000-0003-0665-7794)

Joseph D. Conroy (email: joseph.conroy@dnr.state.oh.us) (https://orcid.org/0000-0002-9561-7294)

Lars G. Rudstam (email: rudstam@cornell.edu) (https://orcid.org/0000-0002-3732-6368)

Peter F. Craigmile (email: pfc@stat.osu.edu) (https://orcid.org/0000-0002-9212-3950)

Doran M. Mason (email: doran.mason@noaa.gov) (https://orcid.org/0000-0002-6017-4243)

Stuart A. Ludsin (email: ludsin.1@osu.edu) (https://orcid.org/0000-0002-3866-2216)

Abstract

The inclusion of unwanted targets in hydroacoustic surveys biases estimates of fish abundance. Thus, knowledge of frequency-dependent responses of unwanted targets (e.g., pelagic macroinvertebrates) can help ensure that transducer frequencies are used that minimize this bias. We determined how fish density estimates varied across multiple frequencies when the larval stage of a midge, *Chaoborus*, was present in the water column. We hypothesized that fish density estimates would increase with increasing transducer frequency, owing to greater backscattering by *Chaoborus* at higher frequencies than lower ones, which allows it to be included with the backscattering caused by fish. We found that fish density estimates were always greater at higher frequencies (e.g., 120 and 200 kHz) compared to a lower one (70 kHz) in several productive north-temperate reservoirs. Furthermore, pairwise comparisons of total (i.e., fish plus *Chaoborus*) backscattering showed that significantly more backscattering occurred at higher rather than lower frequencies. We also found that fish density estimates varied between spring and summer, partially owing to inter-seasonal size variation in *Chaoborus* that influenced its backscattering. Beyond demonstrating why the presence of pelagic macroinvertebrates needs to be considered when estimating fish abundance with hydroacoustics, we provide methods to identify and reduce this bias.

Key words: phantom midge, *Mysis,* fish acoustics, *Dorosoma cepedianum*, diel vertical migration, geostatistics

1. Introduction

As with all sampling methods used to estimate fish abundance, hydroacoustic surveys are not without bias. One potential problem is that hydroacoustic surveys do not exclusively detect the targets of interest (i.e., fish). For example, many macroinvertebrates, such as *Mysis* spp. (Rudstam et al., 2008; Axenrot et al., 2009), corixids (Kubecka et al., 2000), chironomids (Kubecka et al., 2000), *Chaoborus* spp. (Knudsen et al., 2006), jellyfish (Colombo et al., 2009), and krill (Simard and Lavoie, 1999) have measurable backscattering at frequencies commonly used during fish hydroacoustic assessment surveys. Therefore, fish abundance estimates could include contributions from non-target organisms, resulting in overestimates of fish abundance (Jurvelius et al., 2008; Rudstam et al., 2008). Owing to the commonality of pelagic macroinvertebrates in small natural lakes (Schindler et al., 1993), the Great Lakes (Beeton, 1960), man-made reservoirs (Chimney et al., 1981), estuaries (Moriarty et al., 2012), and oceans (Atkinson et al., 2004), the need to quantify and understand this bias seems paramount, regardless of ecosystem type.

The degree of bias from pelagic macroinvertebrates can be influenced by the design of the hydroacoustic survey, as well as the behaviors and biological attributes of the macroinvertebrates. Hydroacoustic surveys of fish abundance are routinely conducted at night because fish typically disperse from schools in reduced light, allowing for more precise estimates of fish abundance (Drastik et al., 2009). However, many other (non-fish) organisms, such as bentho-pelagic macroinvertebrates, also often reside in the water column at night. For example, *Mysis* spp. (Rudstam et al., 1989), *Chaoborus* spp. (La Row and Marzolf, 1970), and krill (Cotte and Simard, 2005) engage in diel vertical

71 migration behavior, where individuals reduce predation risk by occupying deeper, darker
72 water (or sediments) during the day and moving into the water column at night to feed
73 and/or find more suitable habitat. Other macroinvertebrates, such as chironomids, also
74 emerge from the benthos during the day and are present in the water column and at the
75 surface at night (Sjöberg and Danell, 1982). Bias from macroinvertebrates is further
76 enhanced by organisms with an air bladder (i.e., *Chaoborus*), which may resonate at
77 certain transducer frequencies and therefore contribute more backscatter than expected
78 based on their size alone (Jones and Xie, 1994; Eckmann, 1998).
79 Not accounting for macroinvertebrates in the water column during a hydroacoustic
80 survey of fish abundance can result in a biased fish estimate. For example, smelt
81 (*Osmerus eperlanus*) density in Lake Hiidenvesi, Finland was overestimated by up to
82 55% when the presence of *Chaoborus* was not considered (Malinen et al., 2005). This
83 bias can be reduced, however, by conducting hydroacoustic surveys using frequencies
84 at which the backscattering from non-target organisms is lower. Knudsen et al. (2006)
85 evaluated the acoustic backscattering response of *Chaoborus* at six different
86 frequencies, ranging 38–710 kHz. These authors detected the greatest response at 200
87 kHz and attributed the higher backscattering at that frequency to resonance by the air
88 sacs of *Chaoborus*. Further, these authors found that the backscattering strength varied
89 with *Chaoborus* size. For this reason, Knudsen et al. (2006) recommended using lower
90 frequencies (e.g., <200 kHz) during fish assessments in the presence of *Chaoborus*.
91 Studies in other ecosystems (e.g., Malinen et al., 2005; Jurvelius et al., 2008; Knudsen
92 and Larsson, 2009) have also concluded that fish abundance estimates measured at

93 200 kHz are biased high when macroinvertebrates (e.g., *Chaoborus*) are present, and
94 that lower frequencies should be used.
95 Herein, we sought to evaluate the potential for a vertically migrating
96 macroinvertebrate, *Chaoborus*, to bias hydroacoustic surveys of fish density in shallow,
97 eutrophic reservoirs common to the eastern United States, as well as provide methods
98 to reduce any observed bias. Specifically, we sampled with 70-, 120-, 200-, and 430-
99 kHz frequencies during two seasons (spring and summer) to identify how estimates of
100 fish density change with frequency in the presence of *Chaoborus*, an abundant
101 organism in these ecosystems. To determine whether backscatter from *Chaoborus*
102 contributed to total acoustic backscatter in our study reservoirs, we first examined the
103 ability of our hydroacoustics system to estimate *Chaoborus* abundance. To further
104 understand the influence of *Chaoborus* on our acoustic surveys, we also: 1) compared
105 total (i.e., both fish and *Chaoborus*) acoustic backscattering (NASC, $m^2 \cdot nmi^{-2}$) from
106 every pairwise combination of frequencies; and 2) determined the frequency-response
107 of reservoir organisms (i.e., both fish and *Chaoborus*) during spring and summer using
108 four different frequencies (70, 120, 200, and 430 kHz). We then evaluated how
109 estimates of fish density varied with transducer frequency and the season sampled.
110 Overall, our findings show frequency-dependent and season-specific biases that should
111 be considered when developing hydroacoustic assessment protocols to estimate fish
112 abundance in the presence of pelagic macroinvertebrates such as *Chaoborus*.
113

2. Methods

2.1 Study ecosystems and species

We conducted mobile hydroacoustic surveys and trawled for fish at night to estimate fish density in three Ohio (USA) reservoirs (i.e., Acton Lake, Alum Creek Lake, and Hoover Reservoir; Figure 1) during spring (May or June) and summer (August) of 2017. As with other Ohio reservoirs, our three study ecosystems are small, shallow, warm, and biologically productive (Table 1), and have seasonal hypolimnetic hypoxia during the summer through early fall. The high productivity of these reservoirs stems from their agricultural- and urban-based watersheds (Vanni et al., 2005).

These reservoirs support a fish community consisting of piscivores and planktivores. Top predators in these reservoirs are typified by largemouth bass (*Micropterus salmoides*) and saugeye (*Sander vitreus canadensis*), with their forage base primarily composed of planktivorous fishes, including gizzard shad (*Dorosoma cepedianum*), crappies (*Pomoxis* spp.), sunfishes (*Lepomis* spp.), and brook silverside (*Labidesthes sicculus*). The main species of interest for this study was gizzard shad (*Dorosoma cepedianum*), which has historically been the most abundant prey species in Ohio reservoirs (Sieber Denlinger et al., 2006; Hale et al., 2008; Dillon et al., 2019).

All of our study reservoirs have populations of the vertically migrating, macroinvertebrate *Chaoborus punctipennis*. *Chaoborus* tend to reside in bottom sediments during daylight hours and move into the water column at night (La Row and Marzolf, 1970). When in the water column at night, resonance from their air sacs holds the potential to contribute to total backscattering estimates, which has been shown to bias estimates of fish density in other ecosystems (e.g., Malinen et al., 2005; Knudsen

et al. 2006). Because this potential bias from *Chaoborus* has not been measured or considered in annual hydroacoustic surveys of fish abundance by the Ohio Department of Natural Resources – Division of Wildlife (ODNR-DOW), which oversees fisheries management in Ohio reservoirs, the need to estimate this bias is paramount (JDC, co-author, ODNR-DOW, pers. comm.)

2.2 Abiotic data collection

Contemporaneously to hydroacoustic surveys and trawls (see sections 2.3 and 2.4), we collected abiotic data at three sites (Figure 1) to inform reservoir condition at the time of fish sampling. Vertical profiles of temperature (nearest 0.1 °C) and dissolved oxygen concentration (nearest 0.1 $mg \cdot L^{-1}$) were determined with a multi-parameter sonde (Model 6600, YSI, Inc., Yellow Springs, Ohio, USA) at 1-m depth increments from the surface to the bottom at each site (n = 3) in each reservoir.

2.3 Hydroacoustic survey design

Hydroacoustic data were collected with a BioSonics echosounder (DT-X; Seattle, Washington, USA) operating four split-beam transducers with different frequencies: 70-kHz transducer (6.5 °, 3 dB beam angle; 3.7 m, 2x near-field); 120-kHz transducer (7.2 °, 3 dB beam angle; 1.7 m, 2x near-field); 200-kHz transducer (6.9 °, 3 dB beam angle; 1.1 m, 2x near-field); and 430-kHz transducer (6.9 °, 3 dB beam angle; 0.6 m, 2x near-field). Even though each frequency transducer had a different near-field distance, the same exact portion of the water column was used within each analysis to enable fair comparisons across frequencies (see sections 2.5-2.7). For every survey, all transducers were oriented downward on a fixed plate secured to the side of the boat, and positioned 0.5 m below the water surface.

160 Hydroacoustic data collection followed procedures outlined in Dillon et al. (2019).
161 Settings included a –130 dB threshold, 0.2-ms pulse duration, pulse rate of 10 pings·s^{-1},
162 start range of 1 m, and a stop range that varied with reservoir depth. Surveys were
163 conducted (depth permitting) in a zig-zag pattern (Figure 1). All mobile surveys began
164 0.5 h after sunset, were conducted at a speed of 7 km·h^{-1} or slower, and were
165 completed at least one hour before sunrise. We collected passive data at night for the
166 length of one transect while moving at survey speed to quantify background noise in
167 each reservoir (Parker-Stetter et al., 2009; Dillon et al., 2019). In our reservoirs, mean
168 volume backscattering strength (S_v in dB) noise ranged -119.2 to -91.5 dB, whereas
169 target strength (TS in dB) noise ranged -148.5 to -99.8 dB.
170 We calibrated each transducer with a frequency-specific standard tungsten-
171 carbide reference sphere of known TS (38.1 mm diameter for 70 kHz; 38.1 mm
172 diameter for 120 kHz; 36 mm diameter for 200 kHz; 17.5-mm diameter for 430 kHz;
173 Foote et al., 1987) during spring and summer. Calibration offsets were then applied to
174 the survey data based on the results from the closest date of field calibration (typically
175 within one month). Using the equations of Del Grosso and Mader (1972) and Francois
176 and Garrison (1982), we calculated speed of sound and absorption coefficients using
177 the average temperature from the entire water column at the deepest site sampled in
178 each reservoir.

179 **2.4 Biological collections**

180 We collected fish for species identification and total length (TL) measurements by
181 towing (at 12–14 km·h^{-1}) a 1-m high x 2-m wide neuston net (6,350-µm mesh) at the
182 surface, and a 1-m high x 1-m wide framed trawl (3,175-µm mesh) at the surface and at

183 specific depths. Depths of sub-surface tows were chosen based on the greatest
184 apparent abundance of fish (i.e., observed backscatter) observed in the concurrent
185 hydroacoustic survey. Individual fish collected with surface net tows may not directly
186 match those sampled by hydroacoustics at deeper depths. However, for the reasons
187 outlined in Dillon et al. (2019), we are justified in the use of our surface net tows, as
188 their main purpose was to collect as many individuals as possible. We conducted three
189 tows with each net in each reservoir, with our net sampling spanning a distance of
190 approximately 500 m (Figure 1). All captured individuals were euthanized, preserved in
191 95% ethanol, and returned to the laboratory where they were identified to species and
192 measured. We measured TL (nearest 1 mm) and wet mass (nearest 1 g) for a subset of
193 up to 50 randomly selected individuals per species per trawl.
194 We collected *Chaoborus* with a pump (TD5-300, Tsurumi Pump, Glendale
195 Heights, Illinois, USA) at the same three sites sampled for abiotic data in each reservoir
196 (Figure 1). *Chaoborus* were sampled at three discrete depths, with the depth of each
197 sample chosen based on site-specific temperature and dissolved oxygen profiles such
198 that individuals were collected in the epilimnion, metalimnion, and hypolimnion (Dillon et
199 al., in review). Each pump sample filtered approximately 1 m^3 of water. Up to 25
200 randomly selected individuals from each discrete-depth sample at each site were
201 measured (nearest 0.1 mm), and lengths were converted to dry mass (nearest 0.001
202 mg) using an established regression (Chimney et al., 2007). Total *Chaoborus* biomass
203 was calculated by multiplying the density of the sample by the average dry mass of the
204 measured individuals. We tested for differences in mean length between *Chaoborus*
205 captured during spring (May or June) and summer (August) with a Mann-Whitney U

206 Test, as Bartlett's Test and visual examination of the data (histograms and Q-Q plots)
207 revealed that the data were non-normally distributed.

208 **2.5 Hydroacoustic estimates of *Chaoborus***

209 To determine whether backscatter from *Chaoborus* contributed to total acoustic
210 backscatter in our study reservoirs, we first examined the ability of our hydroacoustics
211 system to estimate *Chaoborus* abundance. To do this, we developed a relationship
212 between a commonly used hydroacoustic index of biomass, S_v, and the pumped
213 biomass estimate of *Chaoborus* by matching the same layer of the hydroacoustic
214 survey to the same layer of the discrete-depth pump sample. Data from additional, but
215 similar, sampling used to complete this analysis (section 2.5) is described in Appendix
216 C.

217 2.5.1 Hydroacoustic processing

218 All hydroacoustic analyses were conducted in Echoview (Versions 7.1–8, Myriax
219 Pty Ltd, Hobart, Tasmania, Australia) following the methods outlined in Dillon et al.
220 (2019), which we briefly describe here. Estimates of background noise at 1-m depth
221 were calculated using equations from Parker-Stetter et al. (2009) and then subtracted
222 from the survey data in the linear domain. We also removed other instances of noise
223 (i.e., from boat wakes, bubbles, methane gas, etc.) by manually scanning the
224 echograms and delineating these areas as "bad data" in Echoview.

225 We used the hydroacoustic data from the 70-, 200-, and 430- kHz frequencies to
226 estimate the abundance of *Chaoborus* through a masking technique similar to one used
227 by Rudstam et al. (2008), who separated echoes of a diel migrating invertebrate (*Mysis*
228 spp.) from that of fish in Lake Ontario. First, a fish-exclusion threshold was applied to

229 the 70-kHz data (Rudstam et al. 2008). Only data from the 70-kHz frequency was
230 thresholded for this analysis, as this frequency: 1) included the smallest acoustic
231 contribution from *Chaoborus* (Knudsen et al., 2006; this study); 2) was used as the
232 frequency that produced the most reliable estimate of fish density (see Results); and 3)
233 was used as the frequency for masking fish echoes from the other higher frequencies
234 (see below).

235 The minimum TS threshold (Table A1) was chosen by examining the *in situ*
236 single-target distributions from -75 to -30 dB and selecting a valley in the distribution. If
237 no clear valley was observed in the *in situ* single target distribution, then we chose the
238 minimum TS value by converting TL of individual fish captured in net/trawl tows to TS
239 with a general dorsal-aspect equation (Love, 1977). Single targets were identified using
240 a maximum beam compensation of 6 dB and the settings listed in Dillon et al. (2019). A
241 range-dependent S_v threshold was set 6 dB less than the selected minimum TS value
242 and input as the "Minimum TS threshold" setting in each S_v variable for every reservoir
243 sampled (see Parker-Stetter et al., 2009).

244 Pings between the 70- and either 200- or 430-kHz data were then matched for
245 complete data overlap. In the S_v variable, the data were resampled as 10 data pixels·m^{-1}
246 and dilated to allow masking areas around each fish target. A data range bitmap was
247 then applied to the dilated data, which removed fish targets (and the area immediately
248 around each fish target); we replaced the values in these areas as no data. Results
249 from the bitmap were then applied as a mask over the 200- or 430-kHz S_v data so that
250 only echoes from *Chaoborus* remained.

251 2.5.2 Analysis

252 We examined the relationship between the average pump biomass estimate and
253 the hydroacoustic estimate of *Chaoborus* biomass (S_v) using least-squares linear
254 regression. We developed four predictive models corresponding to the two frequencies
255 (200 and 430 kHz) and seasons (spring: May or June; summer: August) used. We
256 generated separate models for each period, owing to observed *Chaoborus* size
257 differences between sampling seasons. We then used the intercept from these models
258 to determine the TS of 1 g dry wt·m^{-3} of *Chaoborus*. Because of the linearity principle in
259 fisheries acoustics, the slope of the relationship between the $\log_{10}$ of biomass or density
260 and S_v in dB should have a slope of 0.1, if the target size is not density-dependent
261 (Simmonds and MacLennan, 2005). We tested if the slope of each model was
262 significantly different from 0.1 by determining if the 95% CI of the estimated slope
263 encompassed 0.1. When the slope of the model was not significantly different from 0.1,
264 we used the intercept estimates from these models to determine the TS (dB) of 1 g dry
265 wtm^{-3} of *Chaoborus*. If the slope was significantly different from 0.1, we forced the slope
266 of the line to equal 0.1 to get an intercept estimate, and then determined the TS (dB) of
267 1 g dry wtm^{-3} of *Chaoborus*.

268 **2.6 Transducer frequency comparisons**

269 We explored how total backscattering (i.e., from fish and *Chaoborus*) differed
270 among frequencies to help explain any observed differences in estimates of fish density
271 among them. We compared cell-specific total backscattering responses (nautical area
272 scattering coefficient, NASC, m^2·nautical $mile^{-2}$ [nmi^{-2}]) from every pairwise combination
273 of frequencies (i.e., 70, 120, 200, and 430 kHz).

274 2.6.1 Hydroacoustic processing

275 The hydroacoustic data processing differed in some ways from that described in
276 section 2.5. While we subtracted noise estimates from the hydroacoustic data, as
277 above, for the analyses conducted here only, data were not thresholded and we used a
278 horizontal cell size of 250 m and vertical cell size of 2.5 m. This cell size was chosen for
279 these analyses because it is beyond the distance where notable spatial correlation was
280 present in our data (Figures A1–A3), and we were able to smooth over any areas where
281 large fluctuations in the acoustic response might exist. We included all data from the
282 depth of the 70-kHz transducer near-field (as this was the deepest near-field from any
283 frequency transducer sampled) to the bottom exclusion zone (0.2 m off the detected
284 bottom) for these analyses only, as *Chaoborus* were found at all depths in our
285 reservoirs.
286 2.6.2 Analysis
287 Frequency-specific and cell-specific NASC values ($m^2 \cdot nmi^{-2}$) were compared to
288 one another with major-axis regressions (Warton et al., 2006) using the R-package
289 "lmodel2" (Legendre, 2018). In so doing, we could test for common slopes and their fit
290 to a 1:1 line (slope = 1, intercept = 0). A significant ($\alpha = 0.05$) relationship between each
291 pairwise combination of frequencies was tested using data from 99 permutations.
292 Using the same data (i.e., 250- x 2.5- m cell size, noise removed, no
293 thresholding), we identified which frequencies (70, 120, 200, 430 kHz) resulted in the
294 highest backscattering of reservoir organisms (i.e., both fish and *Chaoborus* together)
295 by examining the frequency-response of our data. We determined the frequency-
296 response during both spring and summer to account for potential differences in the
297 frequency-dependent backscattering response associated with changes in organism

298 (i.e., fish and/or *Chaoborus*) size. The frequency-response (± 1 standard error, SE) was
299 calculated as the average cell-specific (from a random selection of one third of the
300 number of cells sampled in each reservoir) acoustic scattering (NASC, $m^2 \cdot nmi^{-2}$) from
301 each frequency sampled.

302 **2.7 Fish density estimation**

303 Only the three lower frequencies (70, 120, and 200 kHz) were used to calculate
304 fish density because they are commonly used in fish abundance assessment surveys
305 used by agencies, including in Ohio (Hale et al., 2008; Godlewska et al., 2009).

306 2.7.1 Hydroacoustic processing

307 Hydroacoustic data processing followed similar methods to those described
308 above (sections 2.5 and 2.6), with noise being removed. Additionally, frequency-specific
309 TS thresholds were applied to the data, using the methods described above (section
310 2.5). We consider thresholding to be the most appropriate method for generating fish
311 density estimates at each frequency, given the high density of *Chaoborus* observed in
312 our ecosystems (Baran et al., 2019), as well as the lack of overlap in TS between
313 known fish and *Chaoborus* at the lower frequencies sampled (see Discussion).

314 Data processing was standardized to 50-m horizontal x 1-m vertical cells within
315 each transect, regardless of transducer frequency or reservoir, and only focused on the
316 1-m vertical interval from 4.2 to 5.2 m. We chose this 1-m depth-layer for analysis as its
317 upper limit (4.2 m) corresponds to the shallowest depth surveyed by the 70-kHz
318 transducer, owing to its 3.7 m, 2x near-field, and position below the water surface, and
319 the lower limit (5.2 m) corresponds to the starting depth of the hypoxic hypolimnion
320 (dissolved oxygen < 2.0 $mg \cdot L^{-1}$), which was present during August surveys (Dillon et al.,

321 in review). We know from previous research that fish avoid hypolimnetic hypoxia in our
322 study reservoirs (Burbacher 2011; Dillon et al., in review). We used Sawada et al.'s
323 (1993) N_v index to identify cells with potentially biased *in situ* TS estimates, owing to
324 overlapping single-target detections, and replaced those cells with the average TS from
325 the same depth-layer (Dillon et al., 2019).
326 2.7.2 Analysis
327 We estimated cell-specific fish density via echo-integration, scaling the area
328 backscattering coefficient (ABC, $m^2 \cdot m^{-2}$) by the average backscattering cross section
329 (σ_{bs}, m^2). Average fish density estimates (number of individuals$\cdot m^{-2}$) were then
330 calculated using a geostatistical model that accounted for the spatial characteristics of
331 our sampling design. Because we used a non-random sampling design (i.e., zig-zag
332 transects; see Figure 1), classical statistical methods are inappropriate, as assumptions
333 about randomized sampling (i.e., independence) were violated (Simard et al., 1992;
334 Petitgas, 2001). By contrast, a geostatistical model-based approach does not require a
335 randomized survey design as it explicitly models inherent spatial trends and correlation
336 in the data (Rivoirard et al., 2000). For this reason, studies have evaluated the efficacy
337 of using geostatistical methods and found that they provide more robust (e.g., more
338 precise variance estimates) estimates of fish abundance than traditional statistical
339 methods (e.g., Petitgas, 2001; Taylor et al., 2005).
340 We describe our geostatistical models (hereafter referred to as spatial models),
341 in brief, with details available in Appendix B. To satisfy assumptions of a Gaussian
342 spatial model, density estimates from every frequency, season (spring or summer), and
343 reservoir sampled were shifted (add 0.5 to each density measurement) and $\log_{10}$

344 transformed. The spatial model included a spatial trend term, as well as an error
345 covariance that assumed an exponential covariance between different locations
346 (measured in km). Our spatial models also included a nugget term in the error
347 covariance, to account for possible measurement error or fine-scale spatial
348 dependencies. Spatial trends were represented by terms for Northing (km), Easting
349 (km), and their interaction, as exploratory data analyses indicated these trends were
350 apparent in our data (PFC and RAD, unpub. data). The spatial model parameters were
351 estimated using maximum likelihood. A spatial model was appropriate for our data
352 analyses, as Akaike information criterion (AIC) analysis indicated preference for spatial
353 models over non-spatial models for most surveys (Supplementary Material; Table S1).
354 Summaries of the spatial models showed that estimates of model terms (i.e., intercept,
355 Northing, Easting, and their interaction), and the significance of these terms varied with
356 the reservoir and season sampled (Supplementary Material: Tables S2–S4). Further,
357 while mean density estimates were similar between the spatial and non-spatial models,
358 the error (SE) estimates from the spatial model were generally smaller than those
359 calculated from the non-spatial model (Supplementary Material: Table S5, Figure S1).
360 Thus, based on the non-random sampling design, the AIC values, and lower observed
361 SE of the estimates, we used the spatial model to calculate average fish density for all
362 of our surveys.
363 To quantify how much the spatially-varying fish density estimates ($\log_{10}$
364 transformed) differed among frequencies and between seasons, we developed a
365 functional analysis of variance (ANOVA) model (Kaufman and Sain, 2010) for each
366 reservoir. We used this approach given that assumptions of independence and equal

367 variances were not met, which precluded the use of a simpler ANOVA. Each functional
368 ANOVA model included a spatial trend (with terms for Northing, Easting, and their
369 interaction), a spatially-varying term for frequency, a spatially-varying term for season,
370 and a spatially-varying term for the errors. We assumed an exponential covariance for
371 each spatially varying term. We only included a nugget term for the error term. The
372 functional ANOVA model was fit using maximum likelihood (see Appendix B for further
373 details).
374

375 **3. Results**

376 **3.1 Fish collections**

377 The majority (by abundance) of the trawl catch was gizzard shad in Acton Lake
378 (100%), whereas brook silverside was caught in greater abundance in Alum Creek Lake
379 (78%) and Hoover Reservoir (74%). The mean TL (± 1 SD) of gizzard shad captured in
380 Acton Lake was 54 ± 19 mm, in Alum Creek Lake was 89 ± 8 mm, and in Hoover
381 Reservoir was 66 ± 18 mm. The mean TL of brook silverside was 52 ± 28 mm in Alum
382 Creek Lake, and 59 ± 15 mm in Hoover Reservoir. The range of fish TLs recorded
383 (regardless of species) was 20–95 mm in Acton Lake, 24–95 mm in Alum Creek Lake,
384 and 30–90 mm in Hoover Reservoir.

385 **3.2 *Chaoborus* collections**

386 Depth-specific pump sampling confirmed the presence of *Chaoborus* in our study
387 ecosystems (Table 2; Figure 2). We captured a wide size-range of *Chaoborus* in
388 conjunction with our hydroacoustic surveys (Table 2; Figure 2). Similar patterns in the
389 mean TL (± 1 SD) of *Chaoborus* were observed across the three reservoirs sampled,

with a higher abundance of smaller *Chaoborus* being captured during summer (3.3 ± 2.1 mm) than during spring (5.9 ± 2.9 mm) (Mann-Whitney test; W = 483380; P < 0.01; Table 2; Figure 2). Further, more individuals were captured during summer (mean density ranged 256 to 688 individuals·m^{-2}) than during spring (mean density ranged 43 to 229 individuals·m^{-2}) in all three reservoirs (Table 2).

3.3 Hydroacoustic estimates of *Chaoborus*

The relationship between the hydroacoustic estimate of *Chaoborus* abundance and the estimate of *Chaoborus* biomass from pump samples varied with the frequency of transducer (200 vs. 430 kHz) and sampling season (Table 3; Figure 3). However, simple least-squares regression results indicated a significant relationship between the hydroacoustic and biomass estimates of *Chaoborus* for every frequency and time period sampled (Table 3). The models with the highest coefficients of determination (R^2 ranged 0.94–0.97) included data from spring (May or June), whereas models from summer (August) had R^2 values that ranged 0.36–0.52 (Table 3). The resultant hydroacoustic portrayal of *Chaoborus* is shown in Figure 4 (right panels).

Estimated slopes of these regression lines ranged 0.05–0.13 (Table 3) and significantly differed from 0.1 for all models. During spring, the TS of 1 g dry wt·m^{-3} of *Chaoborus* was larger at 200 kHz (TS = -21.1 dB) than at 430 kHz (TS = -45.8 dB). The opposite pattern was found during summer, where a larger TS value was observed at 430 (TS = -13.1 dB) than at 200 kHz (TS = -37.2 dB). When all of the data were pooled (between seasons), the overall TS value for 1 g dry wt·m^{-3} of *Chaoborus* was -35.4 dB at 200 kHz and -26.8 dB at 430 kHz.

3.4 Transducer frequency comparisons

413 Pairwise comparisons of total (i.e., from both fish and *Chaoborus*) NASC ($m^2 \cdot nmi^{-2}$)
414 in the same cell between frequencies showed a consistent pattern of more
415 backscattering at higher frequencies (Figure 5). Our analyses revealed significant
416 differences ($P = 0.01$) between total backscattering for every comparison, with the
417 calculated slopes indicating that backscattering was greater at higher frequencies than
418 at lower ones (Table 4). A visual representation of this finding can be seen in our
419 snapshots of the frequency-specific thresholded echograms (Figure 4), where higher S_v
420 values were observed at higher frequencies.
421 The frequency-dependent response of total (i.e., from both fish and *Chaoborus*)
422 NASC was similar among reservoirs, but varied between seasons (Figure 6). During
423 spring (May or June), we observed a hump-shaped curve in the frequency-response,
424 with a peak at 200 kHz. However, during summer (August), we found an increasing
425 trend in the frequency-response, with the echo energy return at 430 kHz almost twice
426 that at 200 kHz (Figure 6). NASC values were highest in Hoover Reservoir during spring
427 and in Acton Lake during summer, with Alum Creek Lake always being the lowest
428 (Figure 6).
429 **3.5 Fish density estimates**
430 Based on the observed increase in area backscattering with frequency (see
431 Figures 4–6), we were not surprised that estimates of average fish density increased
432 with the transducer frequency used during both seasons (Table 5). The average fish
433 density calculated for Acton Lake during August at 200 kHz was 5.1 times greater than
434 at 70 kHz. For Alum Creek Lake, it was 2.6 times greater, and for Hoover Reservoir, it
435 was 3.6 times greater (Table 5). The magnitude of the difference in fish density

436 estimates between 120-kHz and 200-kHz transducers was usually smaller than when
437 comparing density estimates calculated at 70 kHz to either of the two higher
438 frequencies. No clear pattern among frequencies or among reservoirs was evident in
439 observed differences in fish density estimates between spring and summer (Table 5).
440 Generally, the standard error of the fish density estimate increased with increasing
441 frequency during both seasons (Table 5).

442 Results from the functional ANOVA showed that differences in fish density
443 estimates were attributable to multiple factors, with the amount of variance explained by
444 each spatially varying parameter differing among reservoirs (Table 6). Across all three
445 reservoirs, sampling season explained more variance in the fish density estimates than
446 the transducer frequency (comparing partial sill parameters; Table 6). These changing
447 patterns of acoustic backscattering between spring and summer likely represent
448 changing population demographics (e.g., abundance, size distributions) of fish,
449 *Chaoborus*, or both. Interestingly, spatial patterns in the fish density estimates differed
450 among frequencies, as the largest range parameters and correlation at 100 m were
451 found for the frequency term (except the range parameter for Acton Lake; see Table 5).
452 The calculated nugget was similar among reservoirs (see Table 6), which was likely due
453 to measurement error or other small-scale spatial features.
454

455 **4. Discussion**

456 The primary goal of our study was to improve the ability of fishery assessment
457 biologists and researchers to use hydroacoustics to estimate fish density in the
458 presence of pelagic macroinvertebrates that are residing in the water column. Towards

this end, we explored how estimates of fish density varied with hydroacoustic transducer frequency (70, 120, and 200 kHz) and sampling season (spring vs. summer) in three Ohio reservoirs with an abundance of *Chaoborus*, a vertically migrating macroinvertebrate that has air sacs, which resonate much like the air bladder of fish. Collectively, our findings demonstrate that pelagic macroinvertebrates can bias estimates of fish density, especially when a high-frequency transducer (e.g., 200 or 430 kHz) is used, and that the degree of bias is season-dependent, owing to changes in the demographics of *Chaoborus*. Below, we discuss these findings in detail and offer recommendations that can benefit the design and analysis of hydroacoustics assessment surveys of fish populations in the presence of non-target organisms such as *Chaoborus*.

4.1 Bias associated with high-frequency transducers

Our calculated estimates of fish density varied with transducer frequency. At 200 kHz, fish density estimates ranged 1.8- to 5.1-fold greater than those made with a 70-kHz transducer. Estimated fish densities at 120 kHz were intermediate to the 70- and 200-kHz transducers, though most were similar to those at 200 kHz. We attribute the differences in fish density among frequencies to the presence of *Chaoborus* in our study ecosystems. Because our assessment of total (i.e., both fish and *Chaoborus*) backscattering increased with increasing transducer frequency, we recommend using a lower frequency transducer (e.g., 70 kHz) when estimating fish density in the presence of *Chaoborus*. Our findings indicate that doing so would reduce bias, and hence, improve estimates of fish density.

481 Such wide differences in density estimates among frequencies were initially
482 surprising, as recent work has shown that different frequencies can produce similar fish
483 abundance estimates (Godlewska et al., 2009), especially when fish density is low
484 (Guillard et al., 2014; Mouget et al., 2019). However, consideration of the presence of
485 *Chaoborus* in our study ecosystems helps explain the observed differences in estimates
486 of fish density. Previous studies have found that strong backscattering by *Chaoborus*
487 can result in fish estimates that are biased high (see Eckmann, 1998; Malinen et al.,
488 2005; Jurvelius et al., 2008; Knudsen and Larsson, 2009). The ability to calculate bias-
489 free and robust estimates of fish density is important, as it can help understand fish
490 population and food web dynamics, which also explains why it is a top priority for
491 management agencies such as the ODNR-DOW (*sensu* Drastik et al., 2017; Dillon et
492 al., 2019; JDC, ODNR-DOW, co-author, pers. comm.).
493 We are confident in our conclusion that *Chaoborus* is responsible for the
494 discrepancy in fish density estimates across frequencies because no other known
495 macroinvertebrate “scatterers” are known to reside in our surveyed ecosystems. While
496 zooplankton were captured in our discrete-depth pump samples (Dillon et al., in review),
497 Ohio reservoirs are generally characterized by small zooplankton taxa (e.g., Rotifera,
498 *Eubosmina*; Bremigan and Stein, 1994; Vanni et al., 2005) that are unlikely to contribute
499 acoustic backscattering. Furthermore, the larger cladoceran and copepod zooplankton
500 that are present in our reservoirs have been found to contribute negligible amounts of
501 backscatter at the frequencies investigated herein (Northcote, 1964; Frouzova et al.,
502 2004). Instead, we argue that the observed increase in backscattering with increasing
503 frequency resulted from *Chaoborus*, a macroinvertebrate known to migrate into the

504 water column at night, and which also has two pairs of air sacs (Teraguchi, 1975) that
505 likely resonate at the higher frequencies used herein.

506 **4.2 Removal of bias using thresholding**

507 The method that we presented in this study to generate a less-biased estimate of
508 fish density in the presence of macroinvertebrates involved simple thresholding with a
509 low-frequency (70 kHz) transducer. As with many hydroacoustic analysis decisions, our
510 ability to derive a bias-free estimate of fish density in the presence of *Chaoborus* can be
511 viewed as a compromise between excluding backscattering from *Chaoborus*, and
512 including that from fish (Malinen et al., 2001; *sensu* Simmonds and MacLennan, 2005).
513 While other methods to achieve this goal are available in the literature (Eckmann, 1998;
514 Wagner-Dobler and Jacobs, 1988; Malinen et al., 2005; Jurvelius et al., 2008), most of
515 these methods require fish and macroinvertebrates to be separated in space or to have
516 different target strength (TS) distributions (but, see Baran et al., 2019). These
517 conditions, however, were never met for any hydroacoustic survey in our ecosystems.
518 Even though fewer *Chaoborus* were present in the water column during the day
519 compared to at night, we still observed *Chaoborus* at all depths at all times (Dillon et al.,
520 in review). Additionally, the schooling behavior of our main fish species of interest
521 (gizzard shad), precluded us from sampling during the day, as it is established practice
522 to estimate abundance of gizzard shad at night (Vondracek and Degan, 1995).

523 Our method of thresholding to generate a fish density estimate appears robust,
524 as our selection of frequency-specific minimum TS values did not bias the differences in
525 fish density that were observed among frequencies. According to hydroacoustic theory,
526 fish density should increase as TS values become smaller. However, we selected a

527 smaller minimum TS value at 70 kHz than at either 120 or 200 kHz (Table A1). Thus,
528 the higher estimates of fish density observed at either 120 or 200 kHz did not stem from
529 our selection of the minimum TS value, and is more likely attributable to interference
530 from *Chaoborus*. Further, across our reservoirs and both sampling seasons, the largest
531 selected minimum TS value (-61 dB; Table A1) corresponded to an estimated fish total
532 length (TL) of 17 mm (Love, 1977), which is a smaller-sized fish than was captured by
533 our nets. The size-class of fish observed in Ohio reservoirs during the time of sampling
534 (20–95 mm) is not sufficiently different from the known TS of *Chaoborus*; a 20 mm fish
535 (TS = -59.9 dB at 200 kHz and -59.7 dB at 120 kHz; Love, 1977) would be within 6 dB
536 of the TS of *Chaoborus* at both 200 kHz (TS = -60 to -64 dB; Jones and Xie, 1994;
537 Knudsen et al., 2006) and 120 kHz (TS = -64 to -66 dB; Baran et al., 2019). Thus, 200
538 and 120 kHz appear to be *inappropriate* frequencies to use for estimation of fish
539 abundance in the presence of *Chaoborus* (Knudsen et al., 2006; Jurvelius et al., 2008;
540 Knudsen and Larsson, 2009; this study). Further, our transducer comparison identified
541 70 kHz as the frequency with the lowest total backscattering response and thus, most
542 appropriate frequency to use for fish density estimation (of the frequencies tested).
543 Although we only estimated fish density within a 1-m layer of the water column
544 (from 4.2 to 5.2 m depth), we would expect to find the same pattern (i.e., increasing fish
545 density with increasing transducer frequency) had a larger portion of the water column
546 been included in the analysis. We expect this pattern to hold as both gizzard shad and
547 *Chaoborus* abundance are known to be greater at shallower rather than deeper depths
548 at the time of sampling (i.e., at night; Dillon et al., 2019; Dillon et al., in review; JDC,

549 ODNR-DOW, coauthor, unpublished data). Thus, potentially even more bias from
550 *Chaoborus* in fish density estimates would have been observed at shallower depths.
551 Unfortunately, we were constricted to conducting our analyses in a 1-m depth
552 layer, as the acoustic near-field increases with decreasing transducer frequency,
553 reducing the proportion of the water column sampled. In our case, the 2x near-field
554 distance of the 70-kHz transducer was calculated to be 3.7 m, restricting our
555 measurements to waters deeper than 4.2 m (depth location of the transducer plus the
556 2x near-field). Thus, to avoid bias from *Chaoborus*, at least in our ecosystems, our
557 hydroacoustic estimates of fish may be biased low, due to the availability bias of our 70-
558 kHz transducer (i.e., fish occupying depths of the water column that are within the near-
559 field of the 70-kHz transducer). This tradeoff in biases (availability of fish versus
560 *Chaoborus* backscatter) is important to be aware of, even though we have clearly
561 demonstrated the importance of considering bias from *Chaoborus*. We suggest that an
562 unbiased, relative index of fish abundance (i.e., reducing bias from *Chaoborus* by using
563 a 70-kHz transducer) is better than a biased, absolute fish abundance estimate (i.e.,
564 using a 200-kHz transducer that samples a larger portion of the water column), as it
565 would provide a more accurate estimate of fish abundance in the ecosystem. Once the
566 extent of bias from *Chaoborus* in fish density estimates at higher compared to lower
567 frequencies is quantified, as shown in this study, additional steps can then be taken to
568 address the fish availability bias. Two potential solutions that hold the potential to
569 overcome biases associated with the deep near-field associated with low-frequency
570 (e.g., 70 kHz) transducers include: 1) using a transducer with a wide beam angle, which
571 will shrink the near-field of the transducer; or 2) using an upward-facing rather than

572 downward-looking transducer (e.g., Baran et al., 2019). Collectively, these results
573 highlight the need to be mindful of potential tradeoffs (e.g., other biases in fish density
574 estimation) that might emerge when seeking to eliminate biases associated with pelagic
575 macroinvertebrates such as *Chaoborus*. Recognition of these tradeoffs in choosing
576 acoustics gear (i.e., transducers) is applicable to any ecosystem.

577 **4.3 Influence of season on frequency-dependent biases**

578 Interestingly, along with the observed transducer frequency responses, fish
579 density estimates varied with the time period of sampling in our three study reservoirs.
580 This result is not surprising when we consider that *Chaoborus* population demographics
581 (e.g., length distributions, abundances) differed between spring (May or June) and
582 summer (August); average lengths decreased from spring to summer. Our expectation
583 is that these changes would influence estimates of fish density, with scattering at a
584 lower frequency being greater during spring (when *Chaoborus* individuals are large)
585 than during summer (when *Chaoborus* individuals are small). A size-dependent
586 scattering-response of *Chaoborus* is unsurprising, as Knudsen et al. (2006) found that
587 longer individuals had greater mean TS values relative to shorter individuals.
588 Additionally, we found more *Chaoborus* during summer when backscattering was lower,
589 than during spring, suggesting that size is more important than density when accounting
590 for potential biases associated with *Chaoborus* backscattering.

591 Some research (e.g., Knudsen et al., 2006; Wagner-Dobler and Jacobs, 1988)
592 has been skeptical regarding the use of acoustics to estimate *Chaoborus* densities.
593 Contrary to this skepticism, however, we observed a significant relationship between
594 *Chaoborus* biomass calculated from discrete-depth pump samples and the

595 corresponding hydroacoustic estimates of biomass (S_v) in those depth-layers. While this
596 relationship varied with transducer frequency (200 or 430 kHz) and sampling season,
597 the observed predictive relationships were all strong and positive, with R^2 values
598 ranging 0.36–0.97. Collectively, the observed patterns in the frequency-dependent
599 response, combined with our predictive *Chaoborus* hydroacoustic abundance models,
600 provide added confidence that *Chaoborus* are driving variation in estimates of fish
601 density among transducer frequencies. Variation in the frequency-dependent response
602 between spring and summer also indicates that seasonal changes in estimated fish
603 density can arise, not only because of demographic changes in the fish population, but
604 also because of demographic variation in the resident *Chaoborus* population. These
605 findings demonstrate the need to consider the dynamics of *Chaoborus*, or other pelagic
606 macroinvertebrates, when choosing what season to assess the target fish population
607 with hydroacoustics.
608

609 **5. Conclusions**

610 Hydroacoustic estimates of fish density varied considerably across our study
611 ecosystems, owing to both characteristics of the sampling gear used (i.e., transducer
612 frequency) and the resident biota (i.e., *Chaoborus*). The large observed differences in
613 estimates of fish density at different frequencies appear primarily due to the frequency-
614 dependent backscattering response of *Chaoborus*. Specifically, we found estimates of
615 fish density to be 1.8- to 5.1-fold higher with a 200-kHz transducer than with a 70-kHz
616 transducer across our three study reservoirs. We also found that total (i.e., combined
617 fish and *Chaoborus*) backscattering increased with increasing transducer frequency,

618 with the greatest total backscattering always observed at the higher frequencies (200
619 kHz and 430 kHz, depending on the season of sampling). We are confident that
620 *Chaoborus* in the water column is the source of our overestimation of fish density, as we
621 found high *Chaoborus* densities in our study ecosystems, as well as strong correlations
622 between hydroacoustic estimates of *Chaoborus* and observed biomass in pump
623 samples. Overall, we stress the need to consider and reduce bias associated with the
624 presence of pelagic macroinvertebrates such as *Chaoborus* during hydroacoustic
625 surveys, which may change seasonally due to changes in their demographics (e.g.,
626 length, abundance). Because both empirical and theoretical data suggest that small
627 *Chaoborus* individuals resonate less than larger individuals, even when at a high
628 density, we recommend conducting fish abundance surveys during times when
629 *Chaoborus* are small in size, if practical. Additionally, we recommend choosing a low-
630 frequency (e.g., 70 kHz) transducer for sampling fish wherever possible—perhaps
631 mounted in an upward-facing direction in shallow ecosystems— to also help reduce
632 potential bias from vertically migrating *Chaoborus* from the outset. Following these
633 recommendations would offer researchers and fishery management agencies alike a
634 means to generate more robust estimates of fish abundance in ecosystems that also
635 support large populations of pelagic macroinvertebrates.
636

637 **Acknowledgments**

638 This project was funded by the Federal Aid in Sport Fish Restoration Program (F-
639 69-P, Fish Management in Ohio) administered jointly by the United States Fish and
640 Wildlife Service and the Division of Wildlife-Ohio Department of Natural Resources

641 (ODNR-DOW; project FADR79 to SAL, JDC, and RAD). Additional support came from
642 the US National Science Foundation (NSF) under grants NSF-DMS-1407604 and NSF-
643 SES-1424481 (to PFG). Thank you to the many people involved in completing the fish
644 assessments, including staff from the Aquatic Ecology Laboratory and ODNR-DOW.
645 Thanks to the University of Toledo for the use of their 430-kHz transducer. We
646 appreciate the constructive criticism received from one anonymous reviewer, which
647 greatly improved a previous version of this manuscript.

References

Atkinson, A., Siegel, V., Pakhomov, E., Rothery, P. 2004. Long-term decline in krill stock and increase in salps within the Southern Ocean. Nature 432, 100–103.

Axenrot, T., Ogonowski, M., Sandström, A., Didrikas, T. 2009. Multifrequency discrimination of fish and mysids. ICES J. Mar. Sci. 66, 1106–1110.

Baran, R., Tuser, M., Balk, H., Blabolil, P., Cech, M., Drastik, V., Frouzova, J., Juza, T., Koliada, I., Muska, M., Sajdlova, Z., Vejrik, L., Kubecka, J. 2019. Quantification of *Chaoborus* and small fish by mobile upward-looking echosounder. J. Limnol. 78, 60–70.

Beeton, A.M. 1960. The vertical migration of *Mysis relicta* in Lakes Huron and Michigan. J. Fish. Res. Board Can. 17, 517–539.

Bremigan, M.T., Stein, R.A. 1994. Gape-dependent larval foraging and zooplankton size: implications for fish recruitment across systems. Can. J. Fish. Aquat. Sci. 51, 913–922.

Burbacher, E. A. 2011. A mechanistic evaluation of the capacity of Ohio reservoirs to support an introduced pelagic piscivore. Master's thesis. The Ohio State University, Columbus.

Chimney, M.J., Winner, R.W., Seilkop, S.K. 1981. Prey utilization by *Chaoborus punctipennis* Say in a small, eutrophic reservoir. Hydrobiologia 85, 193–199.

Chimney, M.J., Herring, M.K., Bowers, J.A. 2007. Instar determination, length-mass and length-length relationships for the larvae of *Chaoborus punctipennis* Say from a southeastern (USA) cooling reservoir. Fund. App. Limnol. 168, 163–168.

670 Colombo, G.A., Benovic, A., Malej, A., Lucic, D., Makovec, T., Onofri, V., Acha, M.,
671 Madirolas, A., Mianzan, H. 2009. Acoustic survey of a jellyfish-dominated
672 ecosystem (Mljet Island, Croatia). Hydrobiologia 616, 99–111.
673 Cotte, C., Simard, Y. 2005. Formation of dense krill patches under tidal forcing at whale
674 feeding hot spots in the St. Lawrence estuary. Mar. Ecol. Press Ser. 288, 199–210.
675 Del Grosso, V.A., Mader, C.W. 1972. Speed of sound in pure water. J. Acoust. Soc.
676 Amer. 52, 1442–1446.
677 Dillon, R.A., Conroy, J.D., Ludsin, S.A. 2019. Hydroacoustic data-analysis
678 recommendations to quantify prey-fish abundance in shallow, target-rich
679 ecosystems. N. Amer. J. Fish. Manag. 39, 270–288.
680 Drastik, V., Kubecka, J., Cech, M., Frouzova, J., Riha, M., Juza, T., Tuser, M., Jarolim,
681 O., Prchalova, M., Peterka, P., Vasek, M., Kratochvil, M., Mrkvicka, T. 2009.
682 Hydroacoustic estimates of fish stocks in temperate reservoirs: day or night
683 surveys? Aquat. Liv. Res. 22, 69–77.
684 Drastik, V., Godlewska, M., Balk, H., Clabburn, P., Kubecka, J., Morrissey, E., Hateley,
685 J., Winfield, I.J., Mrkvicka, T., Guillard, J. 2017. Fish hydroacoustic survey
686 standardization: a step forward based on comparisons of methods and systems
687 from vertical surveys of a large deep lake. Limnol. Oceanogr. Meth. 15, 836–846.
688 Eckmann, R. 1998. Allocation of echo integrator output to small larval insect
689 (*Chaoborus* sp.) and medium-sized (juvenile fish) targets. Fish. Res. 35, 107–113.
690 Foote, K.G., Knudsen, H.P., Vestnes, G., MacLennan, D.N., Simmonds, E.J. 1987.
691 Calibration of acoustic instruments for fish density estimation: a practical guide.

692 ICES (International Council for the Exploration of the Sea) Cooperative Research
693 Report 144.
694 Francois, R.E., Garrison, G.R. 1982. Sound absorption based on measurements. Part
695 II: Boric acid contribution and equation for total absorption. J. Acoust. Soc. Amer.
696 72, 1879–90.
697 Frouzova, J., Kubecka, J., Matena, J. 2004. Acoustic scattering properties of freshwater
698 invertebrates. Proceedings of the Seventh European Conference on Underwater
699 Acoustics, 319–324.

700 Godlewska, M., Colon, M., Doroszczyk, L., Dlugoszewski, B., Verges, C., Guillard, J.
701 2009. Hydroacoustic measurements at two frequencies: 70 and 120 kHz –
702 consequences for fish stock estimation. Fish. Res. 96, 11–16.
703 Guillard, J., Lebourges-Daussy, A., Balk, H., Colon, M., Jozwik, A., Godlewska, M.
704 2014. Comparing hydroacoustic fish stock estimates in the pelagic zone of
705 temperate deep lakes using three sound frequencies (70, 120, 200 kHz). Inland Wat.
706 4, 435–444.
707 Hale, S.R., Degan, D.J., Renwick, W.H., Vanni, M.J., Stein, R. 2008. Assessing fish
708 biomass and prey availability in Ohio reservoirs. American Fisheries Society
709 Symposium 62, 517–541.
710 Jones, I.S.F., Xie, J. 1994. A sound scattering layer in a freshwater reservoir. Limnol.
711 Oceanogr. 39, 443–448.

712 Jurvelius, J., Knudsen, F.R., Balk, H., Marjomäki, T.J., Peltonen, H., Taskinen, J.,
713 Tuomaala, A., Viljanen, M. 2008. Echo-sounding can discriminate between fish and
714 macroinvertebrates in fresh water. Freshwat. Biol. 53, 912–923.
715 Kaufman, C.G., Sain, S.R. 2010. Bayesian functional ANOVA modeling using Gaussian
716 process prior distributions. Bayesian Anal.. 5, 123–149.
717 Knudsen, F.R., Larsson, P., Jakobsen, P.J. 2006. Acoustic scattering from a larval
718 insect *Chaoborus flavicans* at six echosounder frequencies: Implication for acoustic
719 estimates of fish abundance. Fish. Res. 791, 84–89.
720 Knudsen, F.R., Larsson, P. 2009. Discriminating the diel vertical migration of fish and
721 *Chaoborus flavicans* larvae in a lake using a dual-frequency echo sounder. Aquat.
722 Liv. Res. 22, 273–280.
723 Kubecka, J., Frouzova, J., Cech, M., Peterka, J., Ketelaars, H.A.M., Wagenwoort, A.J.,
724 Papacek, M. 2000. Hydroacoustic assessment of pelagic stages of freshwater
725 insects. Aquat. Liv. Res. 13, 361–366.
726 La Row, E.J., Marzolf, G.R. 1970. Behavioral differences between 3rd and 4th instars of
727 *Chaoborus punctipennis* Say. Amer. Midland Natural. 84, 428–436.
728 Legendre, P. 2018. lmodel2: Model II Regression. R package version 1.7-3.
729 https://cran.R-project.org/package=lmodel2
730 Love, R.H. 1977. Target strength of an individual fish at any aspect. J. Acoust. Soc.
731 Amer. 62, 1397–1403.
732 Malinen, T., Horpilla, J., Liljendahl-Nurminen, A. 2001. Langmuir circulations disturb the
733 low–oxygen refuge of phantom midge larvae. Limnol. Oceanogr. 46, 689–692.

734 Malinen, T., Tuomaala, A., Peltonen, H. 2005. Hydroacoustic fish stock assessment in
735 the presence of dense aggregations of *Chaoborus* larvae. Can. J. Fish. Aquat. Sci.
736 62, 245–249.
737 Moriarty, P.E., Andrews, K.S., Harvey, C.J., Kawase, M. 2012. Vertical and horizontal
738 movement patterns of scyphozoan jellyfish in a fjord-like estuary. Mar. Ecol. Prog.
739 Ser. 455, 1–12.
740 Mouget, A., Goulon, C., Axenrot, T., Balk, H., Lebourges-Dhaussy, A., Godlewska, M.,
741 Guillard, J. 2019. Including 38 kHz in the standardization protocol for hydroacoustic
742 surveys in temperate lakes. Rem. Sens. Ecol. Conserv. 1–14.
743 Northcote, T.G. 1964. Use of a high-frequency echo sounder to record distribution and
744 migration of *Chaoborus* larvae. Limnol. Oceanogr. 9, 87–91.
745 Parker-Stetter, S.L., Rudstam, L.G., Sullivan, P.J., Warner, D.M. 2009. Standard
746 operating procedures for fisheries acoustic surveys in the Great Lakes. Great Lakes
747 Fisheries Commission Special Publication 09–01. Ann Arbor, Michigan.
748 Petitgas, P. 2001. Geostatistics in fisheries survey design and stock assessment:
749 models, variances and applications. Fish. 2, 231–249.
750 Rivoirard, J., Simmonds, J., Foote, K.G., Fernandes, P., Bez, N. 2000. Geostatistics for
751 estimating fish abundance. Blackwell Scientific Publications, Oxford, UK.
752 Rudstam, L.G., Danielsson, K., Hansson, S., Johansson, S. 1989. Diel vertical migration
753 and feeding patterns of *Mysis mixta* (Crustacea, Mysidacea) in the Baltic Sea. Mar.
754 Biol. 101, 43–52.

755 Rudstam, L.G., Knudsen, F.R., Balk, H., Gal, G., Boscarino, B.T., Axenrot, T. 2008.
756 Acoustic characterization of *Mysis relicta* at multiple frequencies. Can. J. Fish.
757 Aquat. Sci. 65, 2769–2779.
758 Sawada, K., Furusawa, M., Williamson, N.J. 1993. Conditions for the precise
759 measurement of fish target strength *in situ*. J. Mar. Acoust. Soc. Jap. 2, 73–79.
760 Schindler, D.E., Kitchell, J.F., He, X., Carpenter, S.R., Hodgson, J.R., Cottingham, K.L.
761 1993. Food web structure and phosphorus cycling in lakes. Trans. Amer. Fish.
762 Soc., 122, 756–772.
763 Sieber Denlinger, J.C., Hale, R.S., Stein, R.A. 2006. Seasonal consumptive demand
764 and prey use by stocked saugeyes in Ohio reservoirs. Trans. Amer. Fish. Soc. 135,
765 12–27.
766 Simard, Y., Legendre, P., Lavoie, G., Marcotte, D. 1992. Mapping, estimating biomass,
767 and optimizing sampling programs for spatially autocorrelated data: case study of
768 the northern shrimp (*Pandalus borealis*). Can. J. Fish. Aquat. Sci. 49, 32–45.
769 Simard, Y., Lavoie, D. 1999. The rich krill aggregation of the Saguenay-St. Lawrence
770 Marine Park: hydroacoustic and geostatistical biomass estimates, structure,
771 variability, and significance for whales. C. J. Fish. Aquat. Sci. 56, 1182–1197.
772 Simmonds, J., MacLennan, D. 2005. Fisheries acoustics: theory and practice. 2n ed.
773 Blackwell Scientific Publications, Oxford, UK.
774 Sjöberg, K., Danell, K. 1982. Feeding activity of ducks in relation to diel emergence of
775 chironomids. Can. J. Zool. 60, 1383–1387.

776 Taylor, J.C., Thompson, J.S., Rand, P.S., Fuentes, M. 2005. Sampling and statistical
777 considerations for hydroacoustic surveys used in estimating abundance of forage
778 fishes in reservoirs. N. Amer. J. Fish. Manag. 25, 73–85.
779 Teraguchi, S. 1975. Correction of negative buoyancy in the phantom larva, *Chaoborus*
780 *americanus*. J. Insect. Physiol. 21, 1659–1670.
781 Vanni, M.J., Arend, K.K., Bremigan, M.T., Bunnell, D.B., Garvey, J.E., Gonzalez, M.J.,
782 Renwick, W.H., Soranno, P.A., Stein, R. A. 2005. Linking landscapes and food
783 webs: effects of omnivorous fish and watersheds on reservoir ecosystems. BioSci.
784 55, 155–167.
785 Vondracek, B., Degan, D. J. 1995. Among- and within-transect variability in estimates of
786 shad abundance made with hydroacoustics. N. Amer. J. Fish. Manag. 15, 933–939.
787 Wagner-Dobler, I., Jacobs, J. 1988. High frequency echography: Quantitative relation
788 between echogram density and vertical distribution of *Chaoborus* larvae. Arch.
789 Hydrobiologia 112, 567–578.
790 Warton, D.I., Wright, I.J., Falster, D.S., Westoby, M. 2006. Bivariate line-fitting methods
791 for allometry. Biol. Rev. 81, 259–291.

792

TABLES

Table 1. Characteristics of the three Ohio reservoirs sampled for this study during 2017. Surface area, average depth (z_{Avg}), and maximum (z_{Max}) depth are reported for the entire reservoir. Total phosphorus concentration (TP) and chlorophyll *a* concentration (Chl*a*) were measured as part of standard Ohio Department of Natural Resources-Division of Wildlife water quality surveys.

Reservoir	Surface area (km^2)	z_{Avg} (m)	z_{Max} (m)	TP (µg·L)	Chl*a* (µg·L)	Survey date
Acton Lake	2.4	3.4	9.5	85.7	57.7	May 30 August 14
Alum Creek Lake	13.5	6.6	19.3	19.8	8.8	May 25 August 28
Hoover Reservoir	11.7	5.7	20.9	40.3	24.4	June 8 August 31

799 **Table 2**. Mean density (# individuals·m^{-2} ± 1 SD) and mean total length (mm ± 1 SD) of
800 *Chaoborus* captured at night in discrete-depth pump samples in Acton Lake, Alum
801 Creek Lake, and Hoover Reservoir (Ohio) during spring (May or June) and summer
802 (August), 2017.
803

Reservoir	Attribute	Spring	Summer
Acton Lake	density	229 ± 14	688 ± 273
	length	7.3 ± 1.8	3.7 ± 2.5
Alum Creek Lake	density	43 ± 52	309 ± 35
	length	4.0 ± 2.9	2.8 ± 1.5
Hoover Reservoir	density	82 ± 28	256 ± 91
	length	6.2 ± 3.0	3.5 ± 2.0

804

805 **Table 3**. Results from least-squares regressions used to quantify the relationship between hydroacoustic estimates of
806 *Chaoborus* acoustic energy (S_v, dB; a proxy for biomass) and *Chaoborus* biomass (log_{10} (g dry wt·m^{-3})) from discrete-
807 depth pump samples collected in three Ohio reservoirs (Acton Lake, Alum Creek Lake, and Hoover Reservoir) during
808 2017. Four regressions (see "Data" column) were conducted corresponding to the two frequencies (200 and 430 kHz) and
809 two seasons (Spring: May or June; Summer: August) of hydroacoustic data collection. We also calculated the target
810 strength (TS, dB) of 1 g dry wt·m^{-3} of *Chaoborus* for each dataset when the slope of the line did not significantly differ from
811 0.1. TS values with an asterisk (*) were calculated after forcing the slope of the regression line for that model (August, 200
812 kHz) to equal 0.1, as the original slope differed from 0.1. Significant terms (α = 0.05) are presented in bold.

Data	Variable	Slope ± 1 SE	P	Overall model	R^2	TS
Spring, 200 kHz	Intercept	**2.11 ± 0.64**	**0.03**	$F_{1, 4}$ = 59.08, P < 0.01	0.94	-21.1
	S_v	**0.08 ± 0.01**	**< 0.01**			
Spring, 430 kHz	Intercept	**4.58 ± 0.68**	**< 0.01**	$F_{1, 4}$ = 115.74, P < 0.01	0.97	-45.8
	S_v	**0.13 ± 0.01**	**< 0.01**			
Summer, 200 kHz	Intercept	0.50 ± 1.11	0.66	$F_{1, 11}$ = 6.11, P = 0.03	0.36	-37.2*
	S_v	**0.05 ± 0.02**	**0.03**			
Summer, 430 kHz	Intercept	1.31 ± 1.33	0.36	$F_{1, 7}$ = 7.57, P = 0.03	0.52	-13.1
	S_v	**0.07 ± 0.03**	**0.03**			

813

814

Table 4. Statistics describing pairwise comparisons (x-axis:y-axis) of frequency-specific (70, 120, 200, and 430 kHz) estimates of total nautical area scattering coefficient (NASC, $m^2 \cdot nmi^{-2}$), calculated with major-axis regression. All slopes were significantly greater than one ($\alpha = 0.05$). NASC includes all scattering after noise was subtracted from the data. Data were not thresholded. CI = confidence interval. All data were collected in three Ohio reservoirs during spring (May or June) and summer (August), 2017.

Comparison	R^2	P	Slope	Slope: 95% CI	Intercept	Intercept: 95% CI
70:120 kHz	0.74	0.01	2.93	2.83, 3.04	3.45	-2.87, 9.39
70:200 kHz	0.79	0.01	3.67	3.56, 3.78	30.49	23.54, 37.04
70:430 kHz	0.38	0.01	8.86	8.23, 9.59	-92.90	-136.32, -55.58
120:200 kHz	0.78	0.01	1.30	1.26, 1.35	16.34	8.84, 23.54
120:430 kHz	0.47	0.01	2.79	2.62, 2.97	-61.85	-95.30, -31.97
200:430 kHz	0.66	0.01	1.87	1.80, 1.96	-32.11	-52.80, -12.77

826 **Table 5**. Statistics from the spatial models used to describe frequency-specific (70, 120, and 200 kHz) estimates of mean
827 fish density (# individuals·m^{-2}) in Acton Lake, Alum Creek Lake, and Hoover Reservoir (Ohio) during spring (May or June)
828 and summer (August), 2017. Thresholds applied are in Table A1. SE = standard error; CI = confidence interval.

		Spring			Summer		
Reservoir	**Frequency**	**Density**	**SE**	**95% CI**	**Density**	**SE**	**95% CI**
Acton Lake	70 kHz	0.38	0.01	0.37, 0.39	0.47	0.01	0.44, 0.49
	120 kHz	0.77	0.03	0.72, 0.82	0.68	0.03	0.63, 0.74
	200 kHz	0.69	0.03	0.64, 0.74	2.40	0.20	2.05, 2.83
Alum Creek Lake	70 kHz	1.06	0.08	0.91, 1.23	0.32	0.00	0.31, 0.33
	120 kHz	1.37	0.07	1.25, 1.51	0.58	0.02	0.54, 0.62
	200 kHz	3.02	0.22	2.62, 3.47	0.84	0.04	0.77, 0.91
Hoover Reservoir	70 kHz	0.69	0.03	0.63, 0.76	0.61	0.02	0.57, 0.64
	120 kHz	1.41	0.04	1.34, 1.48	2.18	0.13	1.93, 2.44
	200 kHz	1.74	0.08	1.60, 1.90	2.19	0.12	1.95, 2.44

Table 6. Results from the functional ANOVA used to determine the difference between fish density estimates (# individuals·m^{-2}; see Table 4) calculated at the three different transducer frequencies (70, 120, and 200 kHz) during two seasons (Spring: May or June; Summer: August) in Acton Lake, Alum Creek Lake, and Hoover Reservoir, 2017. The partial sill indicates the variance accounted for by each spatial term in the functional ANOVA model, and the range parameter and correlation at 100 m show the relationship between the terms in the model and distance. A larger range parameter indicates strong spatial covariance of that term in the model. The estimated nugget term for the error terms are: Acton Lake = 0.23; Alum Creek Lake = 0.12; and Hoover Reservoir = 0.16.

Reservoir	Parameter	Partial Sill	Range Parameter	Correlation at 100 m
Acton Lake	Intercept	<0.01	0.21	0.98
	Season	0.16	0.21	0.62
	Frequency	0.05	0.19	0.58
	Error	0.18	2.38	0.41
Alum Creek Lake	Intercept	0.04	0.15	0.52
	Season	0.21	<0.01	<0.01
	Frequency	0.09	1.59×10^5	1.00
	Error	0.20	0.12	0.27
Hoover Reservoir	Intercept	0.08	0.03	0.05
	Season	0.20	0.04	0.09
	Frequency	<0.01	11.16	0.99
	Error	0.02	5390.01	0.09

FIGURE CAPTIONS

Figure 1. Location of Ohio in North America (A), and the survey design in Acton Lake (B), Alum Creek Lake (C), and Hoover Reservoir (D). The hydroacoustic (solid lines), trawling (dashed lines with circle end caps), and abiotic/discrete-depth pump sampling (squares) sites are displayed on each map.

Figure 2. Length distribution of *Chaoborus* from discrete-depth pump samples collected in Acton Lake, Alum Creek Lake, and Hoover Reservoir (Ohio) during 2017. These data were used to build the predictive models between observed *Chaoborus* biomass and hydroacoustic estimates of *Chaoborus* abundance. Each column represents a different season (Spring: May or June; Summer: August) sampled and each row is a specific reservoir. Sampling in the additional reservoirs is described in Appendix C.

Figure 3. Relationships between hydroacoustic estimates of *Chaoborus* mean volume backscattering strength (Sv), which is a proxy for biomass, and estimated *Chaoborus* biomass (dry wt) in discrete-depth pump samples collected in Acton Lake, Alum Creek Lake, and Hoover Reservoir (Ohio) during 2017. Data are presented from multiple reservoirs, years, times of day, frequencies (200 kHz = left panels; 430 kHz = right panels), and seasons (spring: May or June = top panels; summer: August = bottom panels).

Figure 4. Hydroacoustic echograms showing the mean volume backscattering strength (S_v) of fish and *Chaoborus* at multiple transducer frequencies (70, 120, and 200 kHz for fish; 430 kHz for *Chaoborus*) in Acton Lake (top panels), Alum Creek Lake (middle panels), and Hoover Reservoir (bottom panels) during August 2017. Fish

862 echograms were thresholded with frequency-specific minimum TS values (Table
863 A1). The *Chaoborus* echogram was created by masking fish from the 70-kHz
864 echogram over S_v from the 430-kHz echogram. Columns correspond to transducer
865 frequency, which increase from left to right. The horizontal axis is 250 m in length.
866 Note: the near-field of each transducer is frequency-specific and not indicated on the
867 echograms.
868 **Figure 5.** Relationships between total (i.e., both fish and *Chaoborus*) cell-specific NASC
869 for pairwise combinations of transducer frequencies (70, 120, 200 and 430 kHz)
870 during spring (May or June; black circle) and summer (August; open square) in
871 Acton Lake, Alum Creek Lake, and Hoover Reservoir (Ohio) during 2017. The solid
872 line is the best-fit major-axis regression line for data from both spring and summer.
873 Data were not thresholded, although background noise was removed.
874 **Figure 6**. Frequency-specific (70, 120, and 200 kHz) response of total backscattering
875 (i.e., both fish and *Chaoborus*) in Acton Lake, Alum Creek Lake, and Hoover
876 Reservoir (Ohio) during 2017. Values are mean ± 1 SE NASC from one third of the
877 number of cells sampled in each reservoir at night during spring (May or June) and
878 summer (August). Data were not thresholded, although background noise was
879 removed.
880

881 **Appendix A.**

882 **Table A.1**. The frequency-specific (70, 120, and 200 kHz) fish target strength threshold (TS min; dB) applied in Acton

883 Lake, Alum Creek Lake, and Hoover Reservoir (Ohio) during Spring (May or June) and Summer (August), 2017.

Reservoir	Survey date	TS min: 70 kHz	TS min: 120 kHz	TS min: 200 kHz
Acton Lake	May 30	-61	-60	-63
	August 14	-65	-60	-63
Alum Creek Lake	May 25	-63	-62	-63
	August 28	-63	-62	-63
Hoover Reservoir	June 8	-62	-60	-63
	August 31	-63	-62	-64

A. FIGURE CAPTIONS

Figure A.1. Estimated covariance structure of the geostatistical model for all transducer frequencies (70, 120, and 200 kHz) used to sample fish during May and August 2017 in Acton Lake, Ohio. Except for the 200-kHz transducer in August, the spatial correlation was close to zero at 0.2 km.

Figure A.2. Estimated covariance structure of the geostatistical model for all transducer frequencies (70, 120, and 200 kHz) used to sample fish during May and August 2017 in Alum Creek Lake, Ohio. Except for the 70-kHz and 200-kHz transducer in May, the spatial correlation is close to zero at 0.2 km.

Figure A.3. Estimated covariance structure of the geostatistical model for all transducer frequencies (70, 120, and 200 kHz) used to sample fish in during June and August 2017 in Hoover Reservoir, Ohio. For all frequencies and both months, the spatial correlation was close to zero at 0.2 km.

902 **Appendix B.**

903 **B.1. Spatial modeling of fish abundance**

904 In a given reservoir, we recorded locations $s = (n, e)^T$ in Northing (*n*) and Easting
905 (*e*) coordinates in units of km, measured relative to the centroid of the reservoir. Our
906 spatial domain of interest was $D \subset \mathbf{R}^2$, a contiguous and convex set of locations with a
907 water depth of at least 4 m.

908 Then for a given reservoir, frequency, and season, we had m fish density
909 estimates $(Y(s_i) : i = 1, \ldots, m)$, at locations $s_i = (n_i, e_i)^T$. Then, $Z(s_i) = \log(Y(s) + 0.5)$
910 denoted our shifted and transformed estimates with $Z = \left(Z(s_1), \ldots, Z(s_m)\right)^T$.

911 We assumed that the transformed ($\log_{10}$) density estimates over the region
912 $D, \{Z(s) : s \in D\}$, was a geostatistical process. More specifically, we had $\{Z(s)\}$ as a
913 Gaussian process (GP) with mean μ(*s*) and covariance $C(s, s')$ for locations s and s'
914 in D. The spatial trend model we used at location s was:

915 $$\mu(s_i) = \beta_0 + \beta_1 n_i + \beta_2 e_i + \beta_3 n_i e_i.$$

916 The covariance between locations *s* and *s'* had the form

917 $$C(s, s') = \theta_1 \exp(-d(s, s')||/\theta_2) + \theta_3 I(s = s'), \qquad \text{(B.1)}$$

918 where θ_1 was the partial sill parameter, θ_2 the range parameter, θ_3 the nugget
919 parameter, $I(\cdot)$ the indicator function, and $d(s, s')$ was the Euclidean distance between s
920 and s'.

921 We estimated the trend parameters $\beta = (\beta_0, \beta_1, \beta_2, \beta_3)^T$ and spatial covariance
922 parameters $\theta = (\theta_1, \theta_2, \theta_3)^T$ from the data Z using maximum likelihood methods (e.g.,
923 Cressie, 1991). We used R code (R Core Team, 2018), available from

https://github.com/petercraigmile/GSP, to fit the geostatistical models to each reservoir, frequency, and time period sampled.

B.2. Predicting average fish density

Letting $|D| = \int_{s \in D} ds$ denote the area of D, the average fish density over D, calculated from the geostatistical density process $\{Y(s)\}$ was

$$\frac{1}{|D|} \int_{s \in D} Y(s)\, ds.$$

Using a set of K prediction locations $p_1, \ldots, p_K$ spaced 50 m apart, but restricted to cover D, we estimated this integral using

$$\frac{1}{K} \sum_{k=1}^{K} Y(p_k).$$

However, we do not know the actual values of the process $Y(\cdot)$ at all locations in D. Instead, using our model, we repeatedly obtained predictions of the shifted and $\log_{10}$-transformed process $Z(\cdot)$ at the prediction locations $p_1, \ldots, p_K$, transformed the predictions back to the original scale, and then summarized these simulations.

Then, let $\mu = \big(\mu(s_1), \ldots \mu(s_m)\big)^T$ denote the spatial trend at the data locations, and $\eta = \big(\mu(s_1), \ldots \mu(s_K)\big)^T$ denote the spatial trend at the predicted locations. Let $V = \big[C\big(s_i, s_j\big) : i = 1, \ldots, m, j = 1, \ldots, m\big]$ denote the covariance matrix for the data Z, $P = \big[C\big(p_i, p_j\big) : i = 1, \ldots, K, j = 1, \ldots, K\big]$ denote the covariance matrix at the predicted locations, and $C = \big[C\big(p_i, s_j\big) : i = 1, \ldots, K, j = 1, \ldots m\big]$ denote the covariance between the predicted and data locations.

Then, a prediction of the shifted and log-transformed process at all the prediction locations simultaneously, $\tilde{Z}$, was drawn from a K-variate normal distribution with mean

$$\eta + CV^{-1}[Z - \mu]$$

and covariance

$$P - CV^{-1}C^T.$$

To provide an unbiased estimate of the abundance with measures of uncertainty (SEs and CIs), we repeatedly obtained 1000 sets of predicted values of this process, $\tilde{Z}^{(l)}, l = 1, \ldots, 1000$. Then, $\tilde{Z}^{(l)}(p_i)$ denoted the lth prediction at location p_i and

$$\tilde{Y}^{(l)}(p_i) = \exp\left(\tilde{Z}^{(l)}(p_i)\right) - 0.5$$

was the back-transformed prediction on the original density scale. Our estimate of the average fish density from the lth prediction was:

$$A_l = \frac{1}{K}\sum_{k=1}^{K} \tilde{Y}^{(l)}(p_k).$$

We used the average of the 1000 A_l values as our estimate of the average fish density over D and the standard deviation of the values as our SE for the average fish density over D. We obtained a 95% confidence interval (CI) for the average fish density by using 0.025 and 0.975 quantiles of the A_l values.

B.3. Functional ANOVA model

We used a functional analysis of variance (ANOVA) (Kaufman and Sain, 2010) to model the spatially-varying relationship between frequency and season. While Kaufman

964 and Sain (2010) used a Bayesian framework, we used a frequentist approach, fitting the
965 model in R using maximum likelihood.
966 For each reservoir, we let D denote the spatial domain of interest in the reservoir.
967 We let $i = 1,2$ denote spring (May or June) or summer (August) and let $j = 1,2,3$ denote
968 70, 120, and 200 kHz. We then let $Z_{ij}(s)$ be our shifted and $\log_{10}$ transformed fish
969 density estimate at location $s \in D$. We modeled the following contrasts:
970 $$W_{11}(s) = Z_{12}(s) - Z_{11}(s) \quad \text{(120 kHz minus 70 kHz, spring);}$$
971 $$W_{12}(s) = Z_{13}(s) - Z_{11}(s) \quad \text{(200 kHz minus 70 kHz, spring);}$$
972 $$W_{21}(s) = Z_{22}(s) - Z_{21}(s) \quad \text{(120 kHz minus 70 kHz, summer);}$$
973 $$W_{22}(s) = Z_{23}(s) - Z_{21}(s) \quad \text{(200 kHz minus 70 kHz, summer);}$$
974 with the functional ANOVA model
975 $$W_{ij}(s) = \mu(s) + \alpha_i(s) + \delta_j(s) + \epsilon_{ij}(s), \quad i = 1,2, j = 1,2, s \in D.$$
976 We then defined the different spatially-varying terms in the model. We assumed
977 that the spatially-varying intercept term, $\{\mu(s) : s \in D\}$, was a Gaussian process (GP)
978 with mean $k_\mu(s)$ and an exponential covariance with partial sill $\theta_{\mu,1}$ and range parameter
979 $\theta_{\mu,2}$:
980 $$C_{\theta_\mu}(s, s') = \theta_{\mu,1} \exp\left(-d(s, s')||/\theta_{\mu,2}\right) \qquad \text{(B.2)}$$
981 The mean term $k_\mu(s)$ was used to capture covariate effects over space; again, we
982 included the Northing, Easting, and their interaction.
983 Following Kaufman and Sain (2010), we supposed that the spatially-varying
984 season effect $\{\alpha_i(s) : s \in D, i = 1,2\}$ was a GP, with zero mean and covariance

$$\operatorname{cov}\left(\alpha_i(s), a_{i'}(s')\right) = \begin{cases} \frac{C_{\theta_\alpha}(s,s')}{2}, & i = i'; \\ \frac{-C_{\theta_\alpha}(s,s')}{2}, & i \neq i', \end{cases}$$

where C_{θ_α} was an exponential covariance with partial sill $\theta_{\alpha,1}$ and range parameter $\theta_{\alpha,2}$ (defined similarly to (B.2)). Similarly, we assumed the spatially-varying frequency contrast effects $\{\delta_j(s) : s \in D, j = 1,2\}$ was a GP with zero mean and covariance

$$\operatorname{cov}\left(\delta_j(s), \delta_{j'}(s')\right) = \begin{cases} \frac{C_{\theta_\delta}(s,s')}{2}, & j = j'; \\ \frac{-C_{\theta_\delta}(s,s')}{2}, & j \neq j', \end{cases}$$

where C_{θ_δ} was an exponential covariance with partial sill $\theta_{\delta,1}$ and range parameter $\theta_{\delta,2}$ (defined similarly to equation B.2).

To complete the model, we assumed that the spatially-varying error term $\{\epsilon_{ij}(s) : s \in D\}$ was an independent GP (over i and j) with mean zero and exponential covariance with partial sill $\theta_{\epsilon,1}$, range parameter $\theta_{\epsilon,2}$, and nugget parameter $\theta_{\epsilon,3}$, (defined similarly to equation B. 1)). Note that only the error term $\{\epsilon_{ij}(s)\}$ contained a nugget term to account for possible measurement error, or short-range spatial effects.

References

Cressie, N. 1991. Statistics for Spatial Data (Revised edition). John Wiley & Sons, New York, NY.

Kaufman, C.G., Sain, S. R. 2010. Bayesian functional ANOVA modeling using Gaussian process prior distributions. Bayes. Analy. 5, 123–149.

R Core Team. 2018. R: A Language and Environment for Statistical Computing. R Foundation for Statistical Computing, Vienna, Austria. URL https://www.R-project.org/.

Appendix C.

To develop our hydroacoustic method to estimate *Chaoborus* abundance, we supplemented the data collected during 2017, as described in this study, with additional collections. Specifically, we also conducted hydroacoustic surveys and trawling during the day (as well as at night) for the reservoirs and dates that were described in the main text (section 2.1). Alum Creek Lake and Hoover Reservoir were also sampled in their entirety at night during August 2016, not just in the lower dam as with our 2017 sampling. An additional four reservoirs were sampled at night during August 2016 and 2017, including Burr Oak Lake, Pleasant Hill Lake, and Findlay #2 Reservoir (Findlay #2 Reservoir was only sampled during 2017). Similar hydroacoustic survey designs (i.e., zig-zag pattern; section 2.3) to the main manuscript were used in all additional reservoirs.

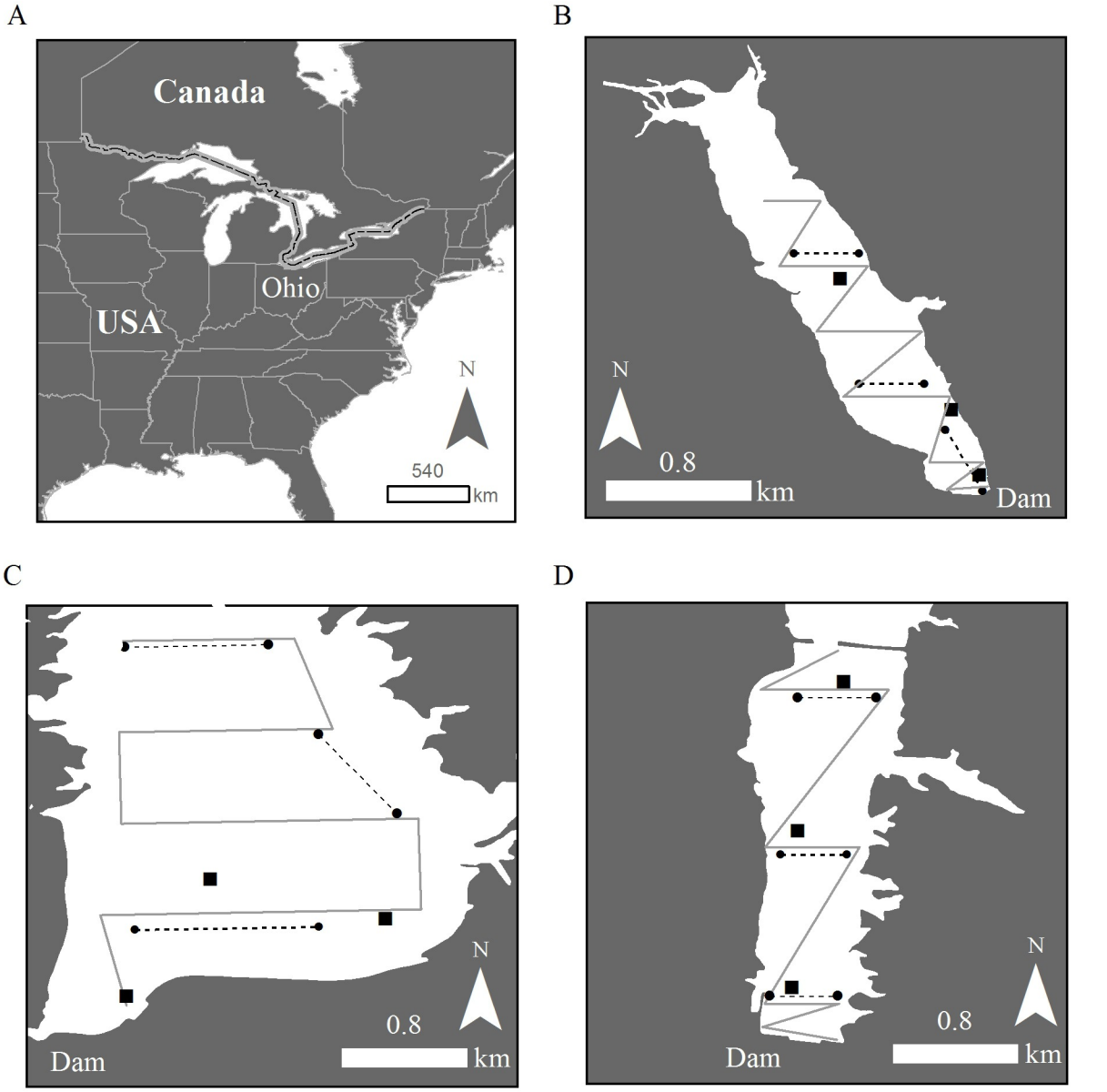
A
Canada
Ohio
USA
N
540
km
B
N
0.8
km
Dam
C
N
0.8
km
Dam
D
N
0.8
km
Dam

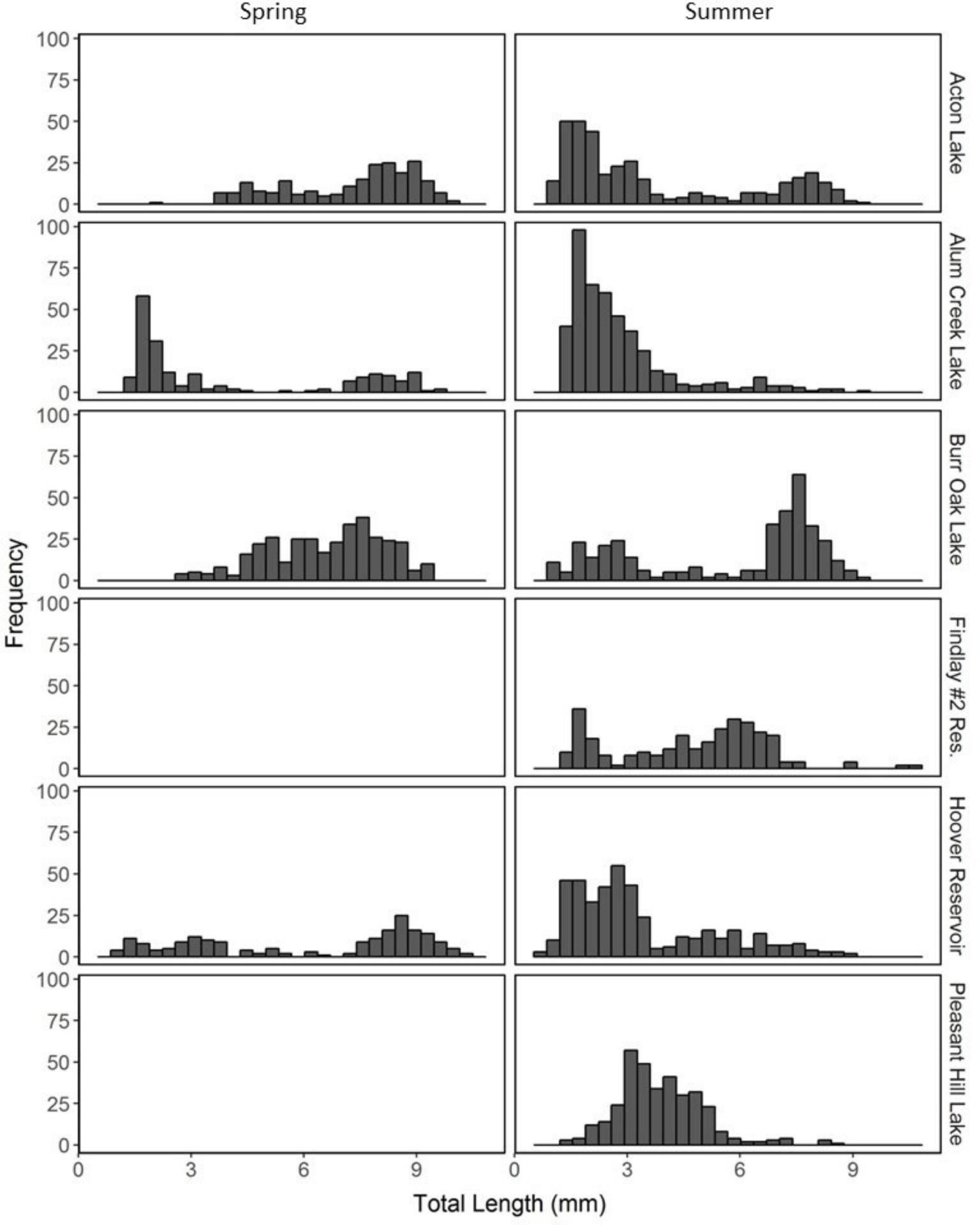
Spring
Summer
Acton Lake
Alum Creek Lake
Burr Oak Lake
Findlay #2 Res.
Hoover Reservoir
Pleasant Hill Lake
Frequency
Total Length (mm)
0
25
50
75
100
0
3
6
9

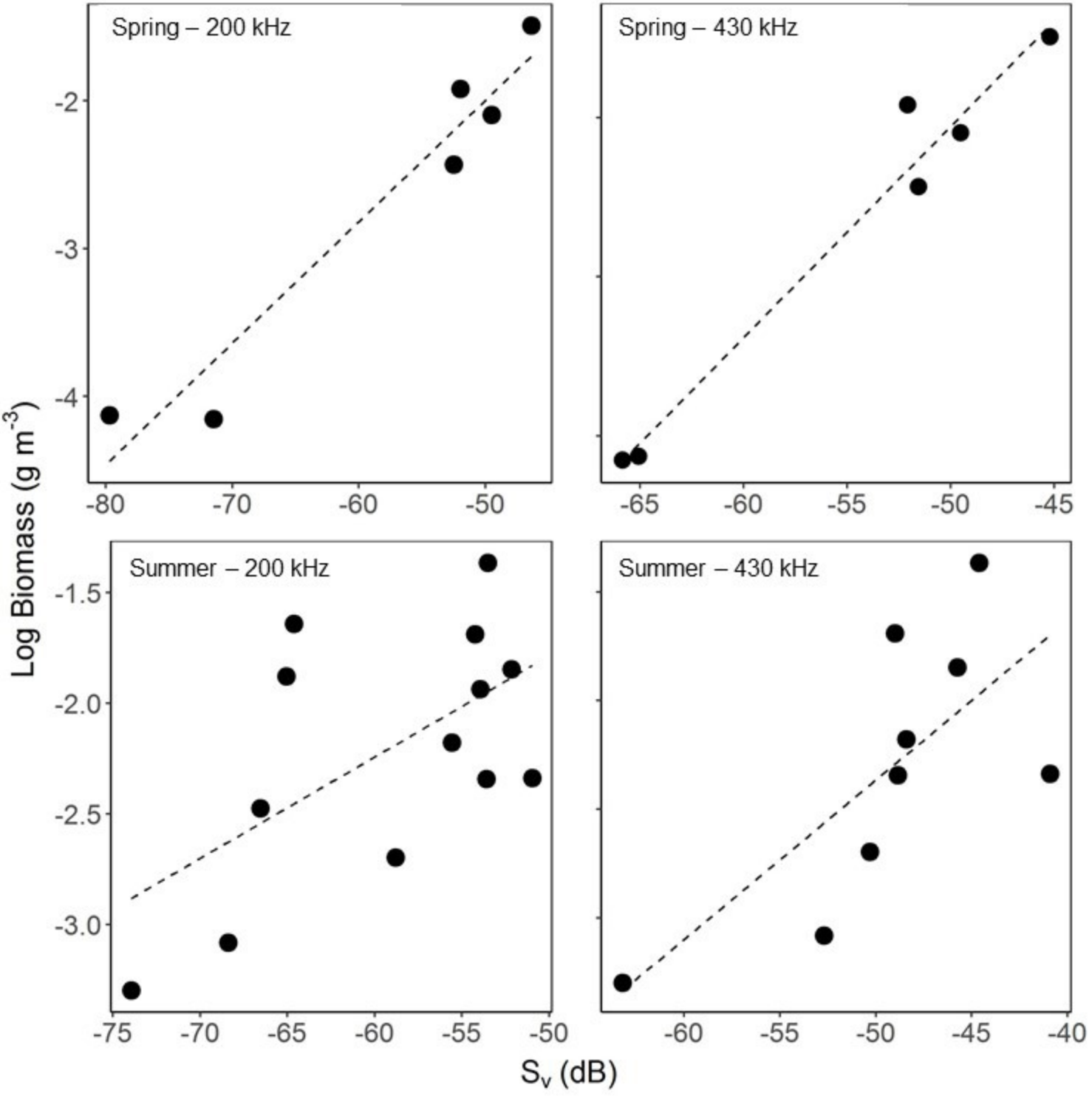
Spring – 200 kHz
Spring – 430 kHz
Summer – 200 kHz
Summer – 430 kHz
Log Biomass (g m-3)
Sv (dB)
-2
-3
-4
-80
-70
-60
-50
-65
-60
-55
-50
-45
-1.5
-2.0
-2.5
-3.0
-75
-70
-65
-60
-55
-50
-60
-55
-50
-45
-40

Fish: 70 kHz

Fish: 120 kHz

Fish: 200-kHz

Chaoborus : 430 kHz

Acton Lake

Alum Creek Lake

Hoover Reservoir

Depth (m)

1
3
5
7
9
3
6
9
12
15
4
7
10
13
16

S_v (dB)

0
-20
-40
-60
-80

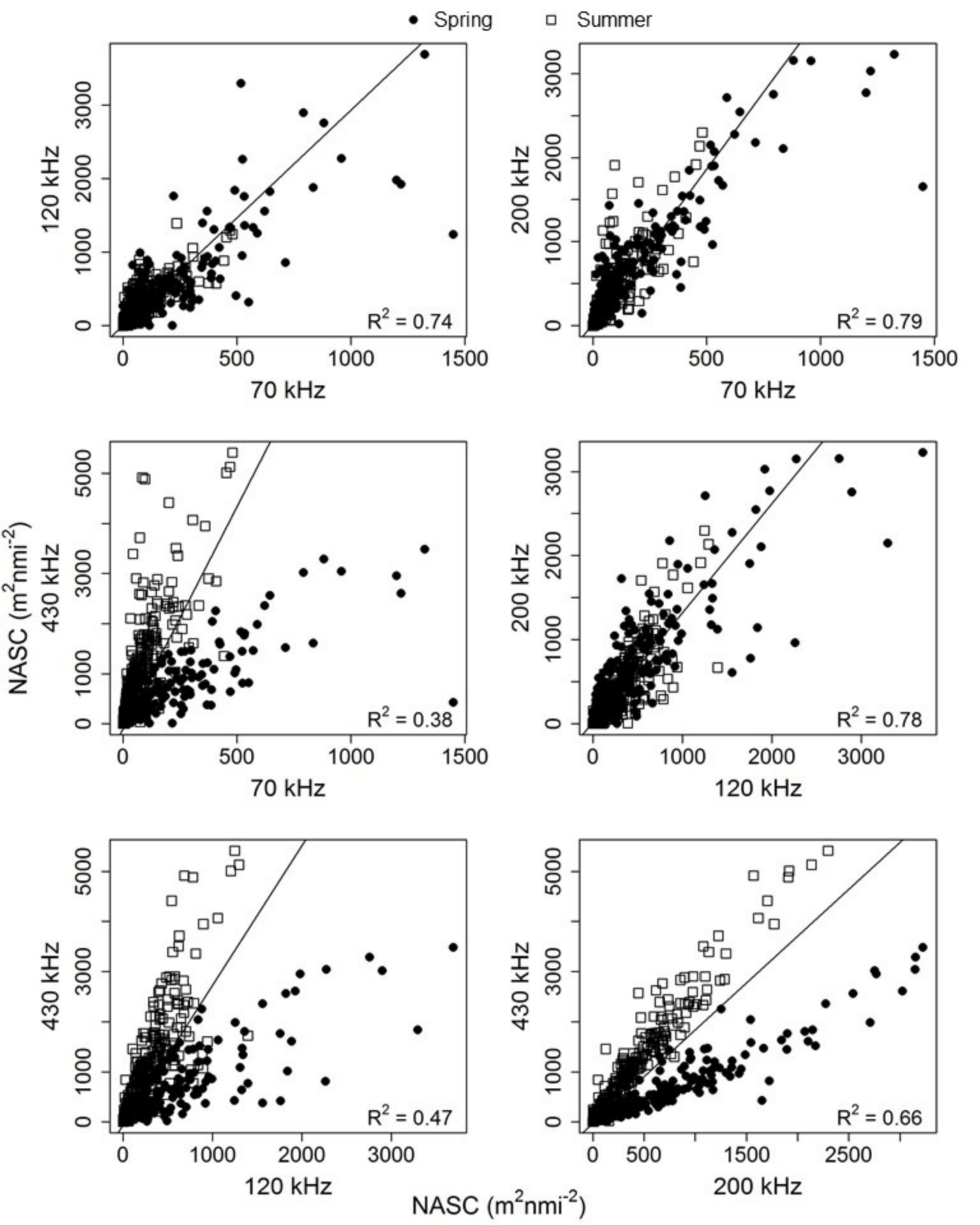
Spring
Summer
120 kHz
70 kHz
R^2 = 0.74
200 kHz
70 kHz
R^2 = 0.79
NASC (m^2nmi^{-2})
430 kHz
70 kHz
R^2 = 0.38
200 kHz
120 kHz
R^2 = 0.78
430 kHz
120 kHz
R^2 = 0.47
430 kHz
200 kHz
R^2 = 0.66
NASC (m^2nmi^{-2})

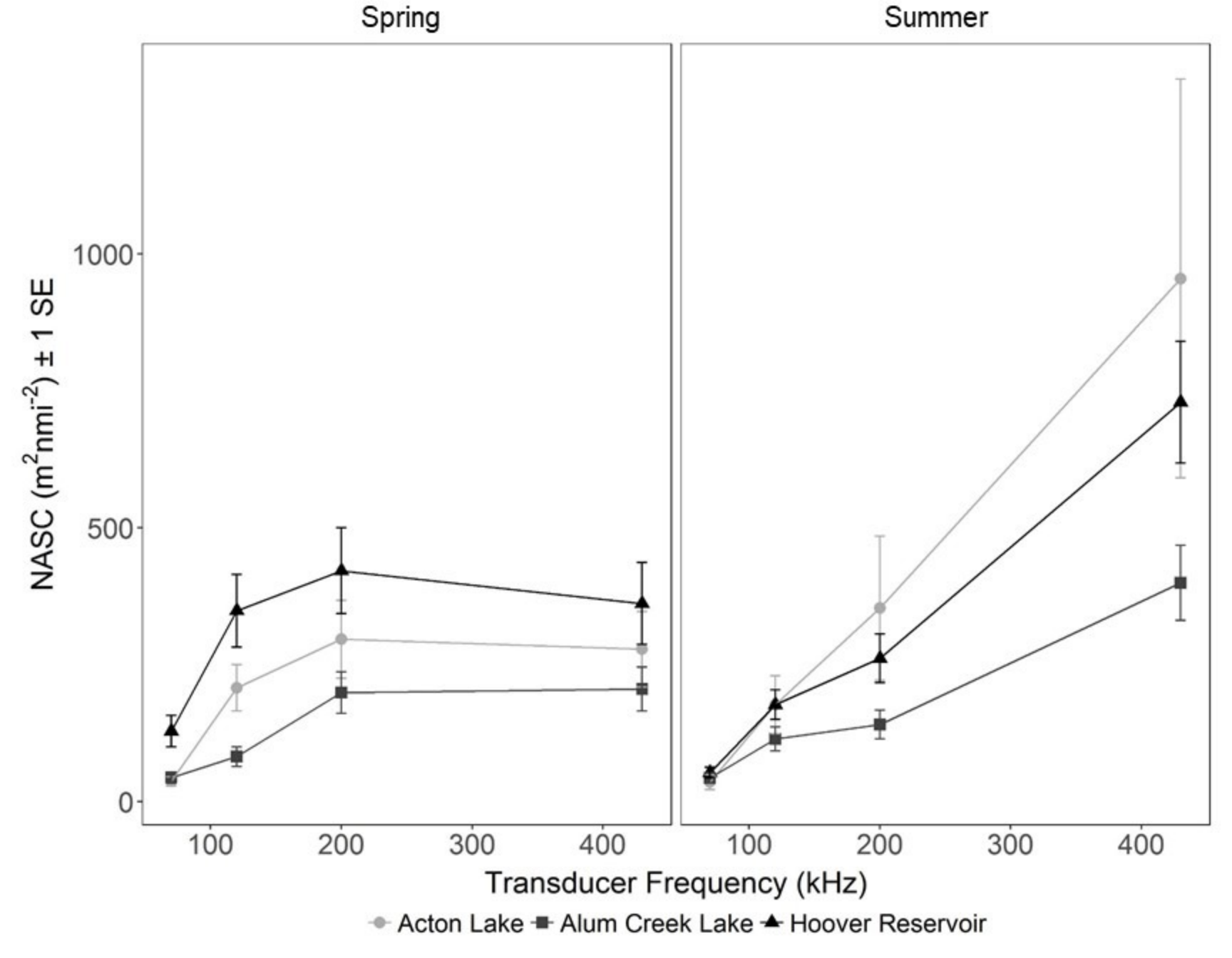
Spring
Summer
NASC (m^2nmi^{-2}) ± 1 SE
0
500
1000
100
200
300
400
Transducer Frequency (kHz)
Acton Lake
Alum Creek Lake
Hoover Reservoir